J|A|C|S
ARTICLES
Published on Web 05/26/2007

Growth Dynamics of CdTe Nanoparticles in Liquid and Crystalline Phases

Marc-Oliver M. Piepenbrock, Tom Stirner, Mary O'Neill,* and Stephen M. Kelly

Contribution from the Departments of Chemistry and Physics, University of Hull, Hull HU6 7RX, United Kingdom

Received January 3, 2007; E-mail: m.oneill@hull.ac.uk

Abstract: Normally the size dependence of the chemical potential is used to explain the growth dynamics of semiconductor nanoparticles. Instead we show that very small CdTe nanoparticles continue to grow at high dilution, the growth rate is virtually independent of monomer concentration, nucleation continues after the growth of larger particles has saturated, and the growth rate has a much greater nonlinear dependence on particle size than predicted by theory. We suggest that nanoparticle growth is fast in the liquid phase and then saturates as the particles change phase from liquid to crystal at a threshold size which depends on the growth temperature and not the monomer concentration. The photoluminescence quantum efficiency becomes high when tellurium is depleted in the reaction solution giving a cadmium enriched surface.

Introduction

II−VI semiconductor nanocrystals have bright and spectrally narrow luminescence, and their optical properties are easily tuned by variation of particle size,[1] making them attractive for a large range of optoelectronic devices such as photovoltaics,[2] light-emitting displays,[3] and biomedical tagging.[4] High quality particles are readily grown by colloidal methods, and classical nucleation theories have been adapted to describe their growth.[5−8] It is normally assumed that nucleated nanoparticles grow by stepwise diffusion of monomers to their surfaces and adsorption thereon. The particle growth rate depends on both the bulk and surface energies and varies with the particle size because of the changing surface area to volume ratio. In particular Ostwald ripening, the growth of particles (crystals or colloidal) at the expense of other particles in the system, has sometimes been used to explain the growth dynamics of nanocrystals and the observed focusing or defocusing in their size distribution.[9,10] Ostwald ripening occurs when smaller particles start to dissolve thus releasing monomers that are then used up by the larger particles. The critical radius, r^*, of a particle which experiences a zero growth rate depends on the monomer concentration in solution, C_b, as a result of the Gibbs−Thomson equation, given by[7]

$$C_b = C_\infty \exp\left(\frac{2\sigma V_m}{r^* RT}\right) \quad (1)$$

where C_∞ is the solubility of a bulk crystal, σ is the surface energy, R is the gas constant, and T is the temperature. The chemical potential of an ensemble of nanoparticles of radius r^* is equal to that of the monomers in solution. A particle of radius, r, dissolves and grows when r is smaller and larger than r^*, respectively. The growth rate is given by[7]

$$\frac{dr}{dt} = \frac{K_D}{r}\left(\frac{1}{r^*} - \frac{1}{r}\right) \quad (2)$$

for diffusion-limited growth and

$$\frac{dr}{dt} = K_R\left(\frac{1}{r^*} - \frac{1}{r}\right) \quad (3)$$

for a first-order reaction controlled process respectively. K_D and K_R are constants. The derivation of eqs 2 and 3 uses only the first two terms of the expansion of the Gibbs−Thomson equation. Hence the size dependence of the chemical potential has been used to explain the dynamics of semiconductor nanoparticle growth.[7,9−15] Yu et al. show that the monomer reactivity is affected by the choice of ligand. They suggest that the chemical potential depends on the effective monomer concentration, which varies with both the monomer concentration and choice of ligand.[16] However Ostwald ripening may not be valid in a binary semiconductor when one of the monomer

(1) Murray, C. B.; Norris, D. J.; Bawendi, M. *J. Am. Chem. Soc.* **1993**, *115*, 8706.
(2) Greenham, N. C.; Peng, X. G.; Alivisatos, A. P. *Phys. Rev. B* **1996**, *54* (24), 17628.
(3) Colvin, V. L.; Schlamp, M. C.; Alivisatos, A. P. *Nature* **1994**, *370* (6488), 354.
(4) Bruchez, M. P.; Moronne, M.; Gin, P.; Weiss, S.; Alivisatos, A. P. *Science* **1998**, *281*, 2013.
(5) Dadyburjor, D. B.; Ruckenstein, E. *J. Cryst. Growth* **1977**, *40* (2), 279.
(6) Lifshitz, I. M.; Slyozov, V. V. *J. Phys. Chem. Solids* **1961**, *19* (1−2), 35.
(7) Sugimoto, T. *Adv. Colloid Interface Sci.* **1987**, *28* (1), 65.
(8) Wagner, C. *Z. Elektrochem.* **1961**, *65* (7−8), 581.
(9) Peng, X. G.; Wickham, J.; Alivisatos, A. P. *J. Am. Chem. Soc.* **1998**, *120*, 5343.
(10) Talapin, D. V.; Rogach, A. L.; Haase, M.; Weller, H. *J. Phys. Chem. B* **2001**, *105* (49), 12278.
(11) Dushkin, C. D.; Saita, S.; Yoshie, K.; Yamaguchi, Y. *Adv. Colloid Interface Sci.* **2000**, *88* (1−2), 37.
(12) Kumar, S.; Nann, T. *Small* **2006**, *2*, (3), 316.
(13) Peng, Z. A.; Peng, X. G. *J. Am. Chem. Soc.* **2002**, *124* (13), 3343.
(14) Talapin, D. V.; Rogach, A. L.; Shevchenko, E. V.; Kornowski, A.; Haase, M.; Weller, H. *J. Am. Chem. Soc.* **2002**, *124* (20), 5782.
(15) Wong, E. M.; Bonevich, J. E.; Searson, P. C. *J. Phys. Chem. B* **1998**, *102* (40), 7770.
(16) Yu, W. W.; Wang, A.; Peng, X. *Chem. Mater.* **2003**, *15*, 4300.

10.1021/ja070032n CCC: $37.00

Table 1. Reaction Conditions and Growth Parameters for Different Batches of CdTe Nanoparticles[a]

batch	temp (°C)	[Cd] (mol L^{-1})	[Te] (mol L^{-1})	*m*(DDA) (g)	*m*(TOP) (g)	*m*(TOPO) (g)	r_0 (nm)	r_1 (nm)	τ_1 (min)
A	140	[0.27]	[0.06]	0.88	4.00	2.00	1.21 ± 0.01	1.79 ± 0.04	0.32 ± 0.04
B	120	[0.27]	[0.06]	0.88	4.00	2.00	1.40 ± 0.02	1.65 ± 0.04	5 ± 0.1
C	160	[0.27]	[0.06]	0.88	4.00	2.00	1.18 ± 0.05	1.9 ± 0.1	0.3 ± 0.07
D	140	[0.27]	[0.27]	0.88	4.00	2.00	1.18 ± 0.05	1.78 ± 0.08	0.4 ± 0.1
E	140	[0.27]	[0.13]	0.88	4.00	2.00	1.40 ± 0.03	1.82 ± 0.07	2.6 ± 0.7
F	140	[0.27]	[0.03]	0.88	4.00	2.00	1.10 ± 0.03	1.76 ± 0.07	0.30 ± 0.05
G	140	[0.27]	[0.01]	0.88	4.00	2.00	1.17 ± 0.02	1.87 ± 0.05	1.5 ± 0.4
H	140	[0.13]	[0.03]	0.88	4.00	2.00	1.05 ± 0.06	1.8 ± 0.1	2.6 ± 0.7

[a] The concentrations refer to the total volume of the DDA, TOP, and TOPO solution.

components is in excess, since the nanocrystal solubility would be different for both. It is also surprising that particles which are in equilibrium with the growth solution do not dissolve in the highly diluted solutions used for optical measurements. In this paper we present extensive experimental evidence to show that the size dependence of the chemical potential does not well explain the size variation of CdTe nanoparticles with time. The same ligands are used for all batches, so that ligand effects need not be considered. An alternative explanation for the observed dynamics is discussed.

Experimental Detail

Since originally suggested by Murray et al.,[1] the tri-*n*-octylphosphine oxide (TOPO), tri-*n*-octylphosphine (TOP) method has become very popular for the preparation of cadmium chalcogenide nanoparticles including CdTe and more recently HgTe.[17−20] This preparation uses dimethyl cadmium ($Cd(Me)_2$) as the cadmium precursor. Unfortunately this material is volatile, highly toxic, unstable, and pyrophoric, and Peng et al. showed that less dangerous cadmium precursors such as cadmium acetate or cadmium oxide can be used to prepare CdSe nanocrystals.[21,22] We use a similar "green" method with a hot injection process to make the CdTe particles. Cadmium(II) acetate dihydrate, TOPO, TOP, dodecylamine (DDA), hexadecylamine (HDA), and tellurium powder were purchased from Aldrich and used as received. Different batches of CdTe were prepared with a wide range of reactant and solvent concentrations and different temperatures as summarized in Table 1. Normally the Cd monomer is in excess. In a typical reaction cadmium(II) acetate dihydrate and DDA were dissolved in TOPO at 140 °C under constant nitrogen flow until a clear solution was obtained. The reaction mixture was stirred at the desired reaction temperature for at least 1 h to ensure complete degassing of the solution. In the meantime tellurium powder was dissolved in TOP at 180 °C until a clear yellow/green solution was obtained (sometimes this solution was slightly cloudy). The resulting TOPTe complex was then injected swiftly into the cadmium precursor solution, and the color changed from clear to yellow usually immediately after injection and further changed from yellow through orange to red over the next few hours indicating the formation and growth of cadmium telluride nanocrystals. Samples were taken at different time intervals after injection (the time of injection was taken as $t = 0$) and diluted by a factor of 180 in toluene for absorption and emission measurements. The particles were characterized by transmission electron microscopy (TEM) and X-ray diffraction (XRD), and the results are included as Supporting Information.

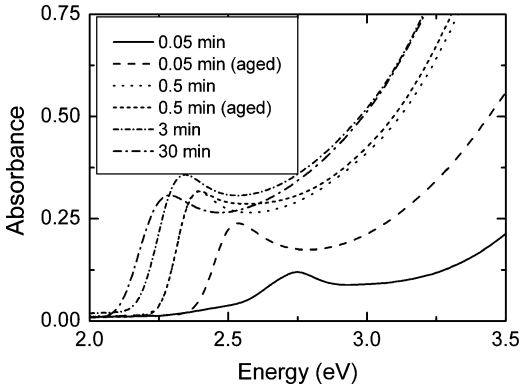

Figure 1. Absorbance of nanocrystals from batch A as a function of growth time. The error in the absorbance is about ±15%. The absorption spectra are from samples withdrawn at specified times. The aged label refers to samples stored in solution at room temperature for 3 days before measurement. The other samples were measured immediately after sampling.

Results and Discussion

Spectrospcopic Analysis of Particle Size. Figure 1 shows the absorbance spectra of the CdTe particles from batch A as a function of reaction time. Some samples were measured immediately and again after aging in the same solution at room temperature for 3 days. Each spectrum shows a clear resonance attributed to the CdTe exciton. The resonance red-shifts with reaction time as the particles grow. Figure 1 also shows that the absorbance of the exciton peak changes significantly with time, and this suggests that the number of nucleated particles also changes with time. Using the method of Yu et al.,[23] we find that the molar concentration of nucleated particles increases with time from $(3.2 \pm 0.6) \times 10^{-4}$ M at $t = 0.05$ min to a maximum value of $(4.6 \pm 0.9) \times 10^{-4}$ M obtained after a reaction time of 10 min. As Table 1 shows, the growth dynamics were investigated for batches having a wide variation of [Te]. However different numbers of particles may be nucleated for the different batches, which would affect the monomer concentration after nucleation. We estimated the number of nucleated particles as a function of the initial monomer concentration from absorbance data obtained after 3 min for the different batches. We found that although the initial [Te] concentration varies by a factor of 27 (from 0.01 to 0.27 M), the number of CdTe particles formed varies by only a factor of 4. Hence the monomer concentration after nucleation is significantly different for the different batches, and we now examine how this affects the particle growth rate.

The energy of the absorption peaks is used to estimate the size of the CdTe nanoparticles via comparison with pseudopo-

(17) Talapin, D. V.; Haubold, S.; Rogach, A. L.; Kornowski, A.; Haase, M.; Weller, H. *J. Phys. Chem. B* **2001**, *105* (12), 2260.
(18) Wuister, S. F.; van Driel, F.; Meijerink, A. *Phys. Chem. Chem. Phys.* **2003**, *5* (6), 1253.
(19) Wuister, S. F.; van Driel, F.; Meijerink, A. *J. Lumin.* **2003**, *102*, 327.
(20) Piepenbrock, M. O. M.; Stirner, T.; O'Neill, M.; Kelly, S. M. *J. Am. Chem. Soc.* **2006**, *128*, 7087.
(21) Peng, X. G. *Chem.—Eur. J.* **2002**, *8* (2), 335.
(22) Peng, Z. A.; Peng, X. G. *J. Am. Chem. Soc.* **2001**, *123* (1), 183.
(23) Yu, W. W.; Qu, L. H.; Guo, W. Z.; Peng, X. G. *Chem. Mater.* **2003**, *15* (14), 2854.

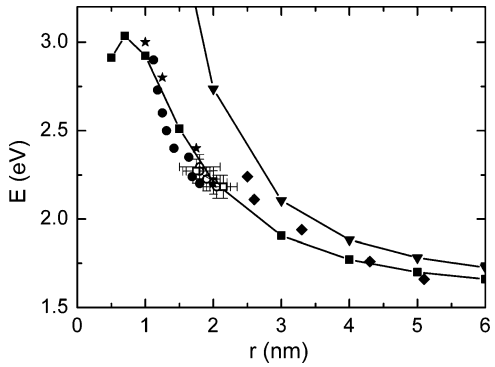

Figure 2. Calculated heavy-hole exciton transition energies of CdTe nanocrystals evaluated by the pseudopotential method (■) and effective mass approximation (▼). The experimental data from TEM images (○) and X-ray diffraction (□) are also shown, as are data points taken from Rajh et al. (★),[25] Masumoto et al. (◆),[26] and Zhang et al. (●).[27] The lines on the calculated plots are a guide to the eye only.

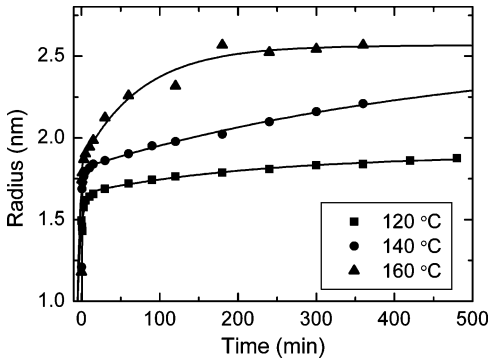

Figure 3. Particle radius versus growth time for CdTe nanocrystals grown at different temperatures. The data points are from experiments, and the lines are empirical fits using eq 4.

tential and effective mass calculations of the variation of band gap with particle size.[24,25] Figure 2 shows the transition energy of the heavy-hole exciton as a function of the quantum dot radius obtained using both approximations. The data points with error bars represent the energies of the exciton peak measured from the absorbance spectra and measured radii from TEM and X-ray experiments. Our data and results from other size studies of CdTe[26−28] agree well with the pseudopotential calculations but not at all with the effective mass approximation. This is not surprising since the pseudopotential calculation includes nonparabolic dispersion of the band-edge states and so provides a better description than the more commonly used effective mass approximation, which breaks down when the exciton diameter is small. A similar discrepancy between predictions of the effective mass approximation and experimental results was also reported by Rajh et al.[26] Both calculations are limited by the assumption of an infinite potential, and closer agreement with experimental results would be expected if the actual confinement of the electrons and holes were considered. This is not possible without a free parameter, since the band offsets between the conduction and valence bands of the semiconductor, and the LUMO and HOMO energies of the stabilizer and solvent are unknown. From Figure 2 it is possible to directly evaluate the particle size from the energy of the principal absorption peak.

Kinetic Analysis of Nanoparticle Growth. Figure 3 shows the nanoparticle radius as a function of growth time for three different growth temperatures. It is clear that there are two distinct growth regimes. Particle growth is initially fast and subsequently slows down. For all samples there appears to be a transition radius at which the growth mechanism changes; the fast processes saturate, and the slower mechanism dominates. We use an empirical model given by

$$r = r_0 + A_1(1 - \exp(-t/\tau_1)) + A_2(1 - \exp(-t/\tau_2)) \quad (4)$$

where r_0 is the radius after nucleation, $r_1 = r_0 + A_1$ and $r_2 = r_1 + A_2$ is the transition radius at which the fast and slow growth processes saturate, respectively. τ_1 and τ_2 are their respective time constants. As Figure 3 shows, eq 4 very well describes the variation of radius with time for all three temperatures. Other growth dynamic curves taken at 140 °C and with different initial Te and solvent concentrations were also modeled and showed the same good agreement. The parameters r_0, r_1, and τ_1 are shown in Table 1 for the different conditions. The time constant for the fast process is extremely short, and the transition radius r_1 is virtually independent of [Te] for samples grown at the same temperature. The parameters r_2 and τ_2 have values in the range 2.1−2.6 nm and 20−400 min for growth at 140 °C with $\tau_2 \gg \tau_1$ in all cases. These latter values have a large error, since the longest measurement time of typically 500 min is less than the saturation time for the slow process. The good agreement of experimental data with eq 4 raises some interesting questions. Why does the fast process saturate so quickly and at a particle size which is virtually independent of monomer concentration? Other authors have attributed a two-stage growth process to the depletion of the monomer and Ostwald ripening.[10,19] As the concentration of the monomer is reduced, the particle comes into equilibrium with its surroundings and approaches a zero growth rate at the transition radius. However the particle ensemble has a distribution of sizes so that subsequent growth is described by Ostwald ripening with the dissolution of the smaller particles in the distribution and the growth of larger particles. This scenario cannot explain the saturation of rapid growth of our particles, since the critical radius, r^*, varies with monomer concentration, whereas the measured transition radius, r_1, is independent of it. We also have experimental evidence for some continued nucleation after saturation. Equation 4 shows that the fast process is effectively complete after a saturation time of $\sim 5t_1$ which is equal to 1.5 min for batch A. However, as shown above, the particle number increases with reaction time up to 10 min, indicating that particles of radii smaller than r_1 continue to grow. Figure 1 provides extra experimental evidence that Ostwald ripening does not explain our observations. The absorption spectra of the aliquot removed at $t = 0.05$ min and diluted by 180 in toluene is measured immediately after injection of the precursor and again after aging in the same solution for 3 days. Surprisingly, despite the high dilution, the NCs continue to grow at room temperature. The absorbance of the exciton doubles after aging indicating a growth in the particle number, and the exciton peak shifts to lower energy, corresponding to a change of particle size from 1.2 to 1.5 nm. This continued growth of small particles on aging in a highly dilute system at room temperature occurs for all reaction conditions and suggests that there can be no Ostwald ripening in the more concentrated

(24) Stirner, T. *J. Chem. Phys.* **2002**, *117*, (14), 6715.
(25) Stirner, T.; Kirkman, N. T.; May, L.; Ellis, C.; Nicholls, J. E.; Kelly, S. M.; O'Neill, M.; Hogg, J. H. C. *J. Nanosci. Nanotechnol.* **2001**, *1* (4), 451.
(26) Rajh, T.; Micic, O. I.; Nozik, A. J. *J. Phys. Chem.* **1993**, *97* (46), 11999.
(27) Masumoto, Y.; Sonobe, K. *Phys. Rev. B* **1997**, *56*, 9734.
(28) Zhang, H.; Yang, B. *Thin Solid Films* **2002**, *418*, 169.

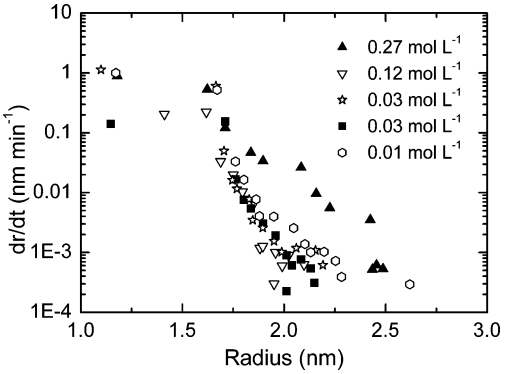

Figure 4. d*r*/d*t* versus radius. The concentration labels refer to [Te]. [Cd] was 0.13 mol L^{-1} for the sample indicated with square data points. Otherwise [Cd] was 0.27 mol L^{-1}.

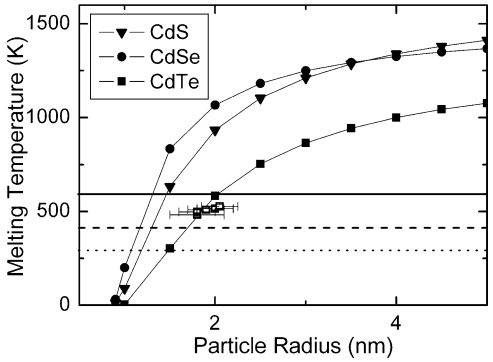

Figure 5. Melting point as a function of radius for different cadmium chalcogenides. The solid black squares are melting points measured for some of our CdTe particles. The horizontal lines denote room temperature (298 K, dotted), the CdTe synthesis temperature (413 K, dashed), and a typical CdSe synthesis temperature (593 K, solid).

growth solutions at the growth temperatures between 393 and 433 K. The supersaturation changes during growth and is lower at the saturation time of $5\tau_1$ than at the sampling time of $t =$ 0.05 min because of late nucleation and particle growth. However the impact of both of these factors can be estimated and are much smaller than the dilution used in the sampling. Hence we can conclude that Ostwald ripening does not determine the transition between the two growth regimes.

We now further probe the effect of concentration on the growth rate and investigate whether a transition from reaction to diffusion controlled dynamics, as proposed elsewhere,[11] can explain the two distinct growth processes of our system. When Ostwald ripening is neglected, i.e., $r^* \rightarrow 0$, eqs 2 and 3 become $dr/dt = K_D/r r^*$ for diffusion control and $dr/dt = K_r/r^*$ for reaction control, respectively. A finite difference approach was used to find d*r*/d*t*, which is plotted as a function of *r* in Figure 4 for the different [Te] concentrations. The particle growth rate is initially high and saturates over a small range of particle sizes to a value over a 1000 times slower. This behavior cannot be explained by a transition between diffusion and reaction controlled processes: both K_D and K_r are proportional to the monomer concentration, and the range over which *r* varies is very small so that both d*r*/d*t* should almost change proportionally as the concentration reduces with particle growth. The inclusion of higher order terms into the expansion of the Gibbs−Thomson equation, which leads to eqs 2 and 3, would not be sufficient to explain the highly nonlinear dependence of d*r*/d*t* with *r*. Indeed, as Figure 4 shows, d*r*/d*t* is virtually independent of [Te] concentration, in contradiction with reaction and diffusion theories, except for batch D, the highest concentration sample where the [Cd]/[Te] is 1:1. This batch had other distinct properties compared to the others, implying a different growth mechanism: TEM showed that the crystals were elongated rather than spherical and the PL quantum efficiency was extremely low. The shape of the d*r*/d*t* versus *r* function is expected from eq 1; there is a rapid saturation from a fast to slow growth rate as a transition radius is approached.

Growth Kinetics Depend on Particle Phase. We have identified some key results describing the kinetics of CdTe NC growth, which the current theories based on the Gibbs−Thomson equation and Ostwald ripening cannot explain. The dynamics are described by two processes with very different time constants. The faster process saturates with a well-defined transition radius which hardly varies with the monomer concentration. Nucleation of some particles continues after saturation, implying a sufficiently high monomer concentration. Particles smaller than a second, smaller critical size continue to grow in highly diluted solutions at room temperature. We now attempt to explain these observations. Quantum dots have a high ratio of surface atoms to bulk atoms giving a size dependent melting point as demonstrated by Goldstein et al. for CdS.[29] The melting point T_r varies with size according to[30]

$$\frac{T_r}{T_0} = \exp\left(-\frac{2(S_m - R)}{3R\left(\frac{r}{3h} - 1\right)}\right) \qquad (5)$$

where T_0 is the bulk melting point, and *R*, the ideal gas constant. The bulk overall melting entropy, $S_m = R[1 + 3\ln(\Theta_s/\Theta_l)]$, with Θ_s, Θ_l denoting the Debye temperatures of the solid and the liquid, respectively. *h* is the average covalent diameter of the Cd and Te atoms. The curves in Figure 5 show the variations of melting point with NC radius for CdTe, CdSe, and CdS. The curve for CdTe was calculated using values for Θ_s and Θ_l taken from a study by Glazov et al.[31] The melting entropy for the CdSe theoretical curve was taken at 14.94 J mol^{-1} K^{-1}.[32] The melting points of CdTe NCs of known size were also measured and plotted in the figure. The experimental data agree well with the theoretical calculations within the small size range that could be evaluated. The horizontal lines in Figure 5 indicate room temperature, the CdTe synthesis temperature (413 K), and a typical CdSe synthesis temperature (593 K). The melting radius of CdTe NCs at 413 K is 1.72 nm which is close to the transition radii shown in Table 1 for the same growth temperature. This suggests that fast growth occurs when the NCs are in a liquid phase and the growth slows down by orders of magnitude when they crystallize. Slightly different transition radii are observed at the different growth temperatures as expected from Figure 4. As mentioned above, extremely small particles continued to grow in highly diluted conditions on aging at room temperature. As illustrated in the Supporting Information, irrespective of the reaction conditions, growth stops at a limiting radius of ~1.5 nm, which corresponds to an exciton transition of 2.5 eV. Indeed this continued growth is only observed when the initial particle

(29) Goldstein, A. N.; Echer, C. M.; Alivisatos, A. P. *Science* **1992**, *256* (5062), 1425.
(30) Zhang, Z.; Zhao, M.; Jiang, Q. *Semicond. Sci. Technol.* **2001**, *16* (6), L33.
(31) Glazov, V. M.; Pavlova, L. M. *Scand. J. Metall.* **2001**, *30* (6), 379.
(32) Jiang, Q.; Li, J. C.; Zhao, M. *J. Phys. Chem. B* **2003**, *107* (50), 13769.

radius is less than 1.5 nm. This is also illustrated in Figure 1, which shows that nanocrystals removed after a growth time of 0.5 min, which have a radius of 1.69 nm, have almost identical absorbance spectra when immediately sampled and after 3 days. Our model can explain the limiting radius of ~1.5 nm above which no room-temperature growth is observed. This value is equal to the room-temperature melting radius shown in Figure 5, so growth also proceeds in the liquid phase at room temperature.

We suggest that the growth of nanoparticles proceeds as follows. Immediately at injection the Cd-precursor monomers (of unknown structure but probably stabilized by DDA and/or TOPO) and Te-precursor (TOPTe) monomers are intimately mixed. These precursor monomers may form a micellar system since they are similar in structure to surfactants with a solvophobic head and a solvophilic tail. These quickly form a population of nuclei, which are too small to be identified by UV−visible spectroscopy since, as Figure 2 shows, the exciton transition energy is >3 eV for droplets with radii < 0.8 nm. An identifiable CdTe exciton absorption band is observed in less than 1 min for all concentrations discussed. The CdTe nanodroplets can grow quickly in the liquid phase since the atoms are mobile and do not have fixed lattice positions. Their size distribution increases with time as will be discussed in detail elsewhere.[33] As shown in Figure 1 there is evidence for continued nucleation in the very early stages of growth. This hardly affects the growth dynamics significantly since particles grow very fast to their transition radius. The mechanism of the nanodroplet growth is unknown and may involve a combination of monomer transfer, nuclei transfer, and coalescence with smaller particles. The latter process is likely in a vigorously stirred solution. The different processes cannot be distinguished kinetically according to their different dependences of particle radius because the kinetics is dominated by the saturation of the growth rate by solidification. On reaching a certain size which depends on temperature, they transform into a truly crystalline state. This could happen as indicated by Sugimoto[7] or Berrettini et al.[34] in a way that the core of the entity becomes crystalline and is covered by a somewhat amorphous shell. Chen et al. report gradual crystallization on an amorphous nanoparticle with a surface reconstruction,[35] but we have no evidence of an amorphous solid here.

Growth in the second phase is very slow (see Figure 3), the size distribution is unchanged with time,[33] and the Te monomer becomes depleted. Inductively coupled plasma spectroscopy (ICP) was carried out on both the isolated crystals and the reactant solution on removal of the nanocrystals. For batch A, the molar concentration of Te in solution saturates quickly after a reaction time of 30 min: [Te] is 2.1×10^{-3} M after 30 min but has reduced to 2.3×10^{-4} M after a reaction time of 120 min, although the radii of the nanocrystals have only grown on average by 0.1 nm. Despite the depletion of the Te monomer, the nanocrystals continue to grow, for batch A to a radius of 2.5 nm after 23 h, and so become more Cd rich. The isolated crystals were measured by ICP after 30, 60, 120, 180, and 240 min, and the ratios of Cd:Te were found to be 1.2:1, 1.3:1, 1.3:1, 1.5:1, and 1.6:1, respectively. Growth in this regime is not related to Ostwald ripening. This is checked by comparing the absorbance before and after aging in a dilute solution for 3 days. A slow dissolution of the nanocrystals in the diluted solution would be expected if Ostwald ripening controlled growth in the reacting solution. The absorbance peak and line width of a sample from batch K grown for 300 min was measured and found not to be affected by dilution and aging.

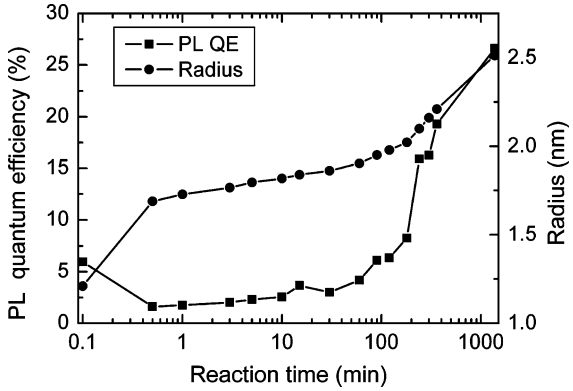

Figure 6. Variation of photoluminescence quantum efficiency and particle radius with time.

Photoluminescence Quantum Efficiency. The PL quantum efficiency (QE) was measured as a function of reaction time, and the results are plotted on a semilogarithmic scale in Figure 6 for batch A. Apart from the first sample, the QE is low when the nanoparticles are in a liquid phase and starts to increase slowly when the particles crystallize. A larger increase of PL is obtained when the Te monomer is depleted and a maximum value of 26.7% is obtained. This suggests that a Cd rich surface provides fewer defects for surface recombination. The PL QE of the other batches increases similarly during the later stages of growth. An exception is batch D where the initial [Cd]/[Te] ratio is 1:1 so that Te depletion is not expected during growth. For this batch, the maximum PLQE obtained was 1.2%. A separation of the nucleation and particle growth rate is normally considered necessary to obtain monodisperse nanocrystals. Despite continued nucleation in the early stages of growth, narrow PL linewidths between 25 and 45 nm were obtained for the nanocrystals. This compares well with values of 23−55 nm obtained elsewhere for CdTe and CdSe nanocrystals.[14,36]

Conclusions

In conclusion we present a large amount of experimental evidence showing that the size dependence of the chemical potential of CdTe nanoparticles has little influence on their growth dynamics: very small particles continue to grow at high dilution, the growth rate is virtually independent of monomer concentration, nucleation continues after the growth of larger particles has saturated, and the growth rate has a much greater nonlinear dependence on particle size than predicted by theory. Instead we suggest that nanoparticle growth is initially rapid in the liquid phase and then becomes very slow above a threshold radius when the particles undergo a phase change from liquid to solid. The measured melting points of CdTe NCs of known

(33) Piepenbrock, M. O. M.; Stirner, T.; Kelly, S. M.; O'Neill, M. In preparation.
(34) Berrettini, M. G.; Braun, B.; Hu, J. G.; Strouse, G. F. *J. Am. Chem. Soc.* **2004**, *126* (22), 7063.
(35) Chen, X. B.; Samia, A. C. S.; Lou, Y. B.; Burda, C. *J. Am. Chem. Soc.* **2005**, *127* (12), 4372.
(36) Qu, L. H.; Peng, X. G.; *J. Am. Chem. Soc.* **2002**, *124* (9), 2049.

size agree well with the theoretical calculations of melting points versus size. We also show that particles continue to grow at room temperature until they have reached a radius of 1.5 nm which closely agrees with the room-temperature melting point. The PL quantum efficiency increases as the surface becomes Cd rich. These observations are relevant to the growth of anisotropic nanocrystals or nanorods. These normally require very high monomer concentrations,[12] often achieved by multiple injections of monomers, so that nucleation continues in the presence of larger nanocrystals. Perhaps small liquid nanodroplets, formed very quickly following nucleation, adsorb preferentially to specific faces of the crystal promoting the growth of rods. We suggest that the quantum efficiency of these systems can be improved by ensuring the depletion of the chalcogen between monomer injections.

Acknowledgment. We thank Gordon Sowersby for technical support. Bob Knight is also acknowledged for ICP results. We acknowledge the EPSRC for funding the research.

Supporting Information Available: TEM images of nanocrystals, X-ray diffraction data, and absorbance spectra illustrating room-temperature growth. This material is available free of charge via the Internet at http://pubs.acs.org.

JA070032N